Syndioselective MMA Polymerization by Group 4 Constrained Geometry Catalysts: A Combined Experimental and Theoretical Study

Yalan Ning,[†] Lucia Caporaso,[‡] Andrea Correa,[‡] Laura O. Gustafson,[†] Luigi Cavallo,*[,‡] and Eugene Y.-X. Chen*[,†]

Department of Chemistry, Colorado State University, Fort Collins, Colorado 80523-1872, and Dipartimento di Chimica, Università di Salerno, Via Ponte don Melillo, I-84084 Fisciano (SA), Italy

Received July 4, 2008; Revised Manuscript Received July 21, 2008

ABSTRACT: This contribution reports a combined experimental (with kinetics and tangible effects on syndioselectivity) and theoretical (with density functional theory) study of (CGC)M catalysts [M = Ti, Zr; CGC = $Me_2Si(\eta^5$-$Me_4C_5)(^t$BuN)], addressing a need for a fundamental understanding of the stereoselectivity observed for such catalysts in polymerization of methyl methacrylate (MMA) and an explanation for the chain-end control nature of the syndioselective MMA polymerization by the chiral (CGC)Ti catalyst. The living/controlled MMA polymerization by (CGC)$TiMe^+MeB(C_6F_5)_3^-$ (**1**) follows the zero-order kinetics in [MMA], implying a faster ring-opening process of the cyclic chelate relative to MMA addition within the catalyst−monomer complex in a unimetallic propagation cycle. The syndioselectivity of **1** is insensitive to monomer and catalyst concentrations as well as to ion-pairing strength varied with counterion structure and solvent polarity. Comparative studies using identical (CGC)M bis(isopropyl ester enolate) structures show that the (CGC)Ti system exhibits noticeably higher syndioselectivity than the isostructural Zr system at ambient temperature. Density functional calculations rationalize the higher syndioselectivity observed for the (CGC)Ti catalyst and lend a theoretical support for the mechanism of MMA- or counterion-assisted catalyst site epimerization after a stereomistake, which accounts for the formation of the predominately isolated *m* stereoerrors.

Introduction

Metallocene complexes, especially those of cationic group 4 complexes,[1] are technologically important, readily accessible, and remarkably tunable catalysts that have been extensively investigated and successfully employed for the production of polyolefins through their catalyzed homogeneous, single-site, (co)polymerization of *nonpolar* vinyl monomers (α-olefins in particular).[2] In comparison, the polymerization of *polar* vinyl monomers with such highly electron-deficient group 4 metallocene and related complexes has been investigated to a much lesser extent.[3] Nonetheless, there is increasing interest in the latter area, with several types of group 4 metallocene complexes being examined for polymerizations of methacrylates,[4−46] acrylates,[41,47−50] acrylamides,[51−54] and methyl vinyl ketone.[55] The polymerization of (meth)acrylates has also been studied computationally.[56−62] Overall, these studies have been focused on the following four major aspects of polymerization: activity/efficiency (catalyst turnover frequency and initiator efficiency), stereospecificity (polymer tacticity and stereocontrol mechanism), control (polymer molecular weight, MW, and molecular weight distribution, MWD, as well as livingness and block copolymer production), and mechanism (kinetics and elementary reactions). Specifically on polymerization stereospecificity, the site-control mechanism enabled the synthesis of highly isotactic poly(methacrylate)s (≥95% *mm*)[9,13,36,44,45] and poly(acrylamide)s (>99% *mm*)[51−54] using chiral C_2-ligated zirconocenium complexes as well as highly syndiotactic poly(methacrylate)s (≥94% *rr*)[4] using chiral C_s-ligated zirconocenium complexes, both at *ambient temperature*. Furthermore, computational studies gained important insights into the stereocontrol mechanism in the polymerization of MMA by C_2-, C_s-, and C_1-ligated chiral *ansa*-zirconocenium complexes.[56,57]

Half-sandwich metal complexes bearing linked (e.g., by the dimethylsilyl group) η^5-cyclopentadienyl (e.g., tetramethyl-substituted Cp)-η^1-amido (e.g., ^{t}BuN) ligands[63] are termed "constrained geometry catalysts", attributing to the phenomenal commercial successes in the production of revolutionary polyolefin materials via (co)polymerization of α-olefins using such group 4 metal catalysts.[64] The C_s-ligated cationic (CGC)Ti alkyl complex, (CGC)$TiMe^+MeB(C_6F_5)_3^-$ (**1**) [CGC = $Me_2Si(\eta^5$-$Me_4C_5)(^t$BuN), Scheme 1], effects *living and syndioselective* polymerization of methacrylates at ambient[18,28] or higher (up to 100 °C)[6] temperatures via an apparent *chain-end control* mechanism. The living and syndioselective features of this catalyst system allowed for the highly efficient (>80% initiator efficiency) synthesis of syndiotactic poly(methacrylate)s at ambient temperature [poly(methyl methacrylate), PMMA, up to 80% *rr*; poly(butyl methacrylate), up to 89% *rr*] with controlled MW and narrow MWD (PDI = M_w/M_n = 1.09) as well as the well-defined, syndiotactic block or random copolymers of methacrylates.[18] The robust (CGC)$TiMe_2/B(C_6F_5)_3$ system (which generates **1** instantaneously) also effectively promotes the polymerization of *n*-butyl acrylate.[47] The corresponding chiral cationic (CGC)Ti ester enolate complex, $\{$(CGC)Ti(THF)[OC(O^{i}Pr)=CMe_2]$\}^+[MeB(C_6F_5)_3]^-$ (**2**, Scheme 1), which simulates the structure of the active propagating species, behaves similarly to that of the (CGC)Ti alkyl complex,[18] producing syndiotactic PMMA (80% *rr*, 18% *mr*, 2.0% *mm*) at ambient temperature with *predominately isolated m stereoerrors* (confirmed by the stereomicrostructure analysis at the pentad level[18]) and again pointing to the apparent chain-end control nature of the polymerization.

In contrast, the isostructural, cationic Zr alkyl complex, (CGC)$ZrMe^+MeB(C_6F_5)_3^-$, is inactive for polymerization of MMA at high or low temperature of polymerization (T_p). However, the cationic (CGC)Zr ester enolate complex, (CGC)Zr(L)[OC(O^{t}Bu)=CMe_2]$\}^+[B(Ar_F)_4]^-$ [**3**, Ar_F = 3,5-$(CF_3)_2C_6H_3$, L = neutral donor ligand such as THF or isobutyrate, Scheme 1], is moderately active and affords,

* Corresponding authors. E-mail: lcavallo@unisa.it; eychen@lamar.colostate.edu.
[†] Colorado State University.
[‡] Università di Salerno.

10.1021/ma801494g CCC: $40.75
Published on Web 09/09/2008

Scheme 1

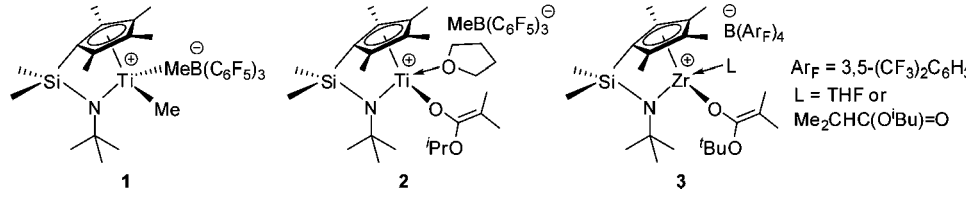

unexpectedly (on the basis of its C_s ligation), highly isotactic PMMA via a site-control mechanism at low T_p: 95.5% *mm* at −60 and −40 °C.[34] Further increasing T_p to −20 °C gave PMMA with a considerably lower isotacticity of 80.5% *mm*. Ambient temperature polymerization results were not given as this cationic (CGC)Zr complex is thermally unstable at $T \geq -20$ °C. A key element in the proposed stereocontrol mechanism for the observed isospecificity of complex **3** is that stereoselective MMA addition occurs predominately at only one of the two enantiotopic lateral sites (i.e., MMA is coordinated to the same lateral Zr site for a site-retention mechanism); this is possible provided that intramolecular 1,4-conjugate Michael addition within the catalyst−monomer complex is fast relative to racemization at Zr by exchange of free and bound MMA and that dissociation of the terminal ester group in the cyclic ester enolate resting intermediate is slow relative to associative displacement (backside attack) by MMA.[34] Apparently, such conditions were met with the polymerization by the in situ-generated **3** in terms of a combination of the low-T_p condition (≤−40 °C) and the use of the oxonium acid activator $H^+(OEt_2)_2[B(Ar_F)_4]^-$ with concomitant delivery of coordinating ligands (diethyl ether and isobutyrate) for the resulting cation upon activation, thereby leading to the production of isotactic PMMA.

As overviewed above, the (CGC)Ti alkyl and ester enolate catalysts **1** and **2** produce syndiotactic PMMA by an apparent chain-end control mechanism at ambient temperature, while the (CGC)Zr ester enolate catalyst **3** affords isotactic PMMA by a site-control mechanism under the low temperature and oxonium acid activation conditions (vide supra). The central objective of the current study is to seek for a fundamental understanding of the stereoselectivity observed for such group 4 catalysts and an explanation for the chain-end control nature of the syndioselective MMA polymerization by the (CGC)Ti catalyst. To this end, we embarked on a combined experimental and theoretical study. Experimentally, we investigated the kinetics of the polymerization by catalyst **1**, examined monomer and catalyst concentration, anion, and solvent effects on syndioselectivity, synthesized the identical (CGC)Ti and Zr bis(ester enolate) complexes, and carried out their comparative studies in MMA polymerization upon activation with three different types of activators at ambient temperature. On the theoretical front, we computed transition states with DFT for MMA additions using both (CGC)Ti and (CGC)Zr catalysts and examined MMA- and anion-assisted site epimerization processes with the (CGC)Ti catalyst.

Experimental Section

Materials, Reagents, and Methods. All syntheses and manipulations of air- and moisture-sensitive materials were carried out in flamed Schlenk-type glassware on a dual-manifold Schlenk line, on a high-vacuum line, or in an argon-filled glovebox. NMR-scale reactions (typically in a 0.02 mmol scale) were conducted in Teflon-valve-sealed J. Young-type NMR tubes. HPLC-grade organic solvents were first sparged extensively with nitrogen during filling 20 L solvent reservoirs and then dried by passage through activated alumina (for Et_2O, THF, and CH_2Cl_2) followed by passage through Q-5 supported copper catalyst (for toluene and hexanes) stainless steel columns. Benzene-d_6 and toluene-d_8 were dried over sodium/potassium alloy and vacuum-distilled or filtered, whereas CD_2Cl_2, and $CDCl_3$ were dried over activated Davison 4 Å molecular sieves. NMR spectra were recorded on either a Varian Inova 300 (FT 300 MHz, ^{1}H; 75 MHz, ^{13}C; 282 MHz, ^{19}F) or a Varian Inova 400 spectrometer. Chemical shifts for ^{1}H and ^{13}C spectra were referenced to internal solvent resonances and are reported as parts per million relative to $SiMe_4$, whereas ^{19}F NMR spectra were referenced to external $CFCl_3$. Elemental analyses were performed by Desert Analytics, Tucson, AZ.

MMA, butylated hydroxytoluene (BHT-H, 2,6-di-*tert*-butyl-4-methylphenol), diisopropylamine, isopropyl isobutyrate, *n*-butyllithium (1.6 M in hexanes), and methylmagnesium bromide (3.0 M in diethyl ether) were purchased from Aldrich Chemical Co. and used as received unless otherwise specified as follows. MMA was first degassed and dried over CaH_2 overnight, followed by vacuum distillation, titration with neat tri(*n*-octyl)aluminum (Strem Chemical) to a yellow end point,[65] and finally distillation under reduced pressure; the purified MMA was stored in a brown bottle inside a glovebox freezer at −30 °C. Diisopropylamine and isopropyl isobutyrate were dried over CaH_2, followed by vacuum distillation. BHT-H was recrystallized from hexanes prior to use. Triflic acid was purchased from Alfa Aesar and redistilled under a nitrogen atmosphere. Tris(pentafluorophenyl)borane, $B(C_6F_5)_3$, trityl tetrakis(pentafluorophenyl)borate, $[Ph_3C][B(C_6F_5)_4]$, and dimethylanilinium tetrakis(pentafluorophenyl)borate, $[HNMe_2Ph][B(C_6F_5)_4]$, were obtained as research gifts from Boulder Scientific Co.; $B(C_6F_5)_3$ was further purified by recrystallization from hexanes at −30 °C, whereas $[Ph_3C][B(C_6F_5)_4]$ and $[HNMe_2Ph][B(C_6F_5)_4]$ were used as received. Tris(pentafluorophenyl)alane, $Al(C_6F_5)_3$, as a 0.5 toluene adduct $Al(C_6F_5)_3\cdot(C_7H_8)_{0.5}$, was prepared by the reaction of $B(C_6F_5)_3$ and $AlMe_3$ in a 1:3 toluene/hexanes solvent mixture in quantitative yield;[66] this is the modified synthesis based on literature procedures.[67] Although we have experienced no incidents when handling this material, *extra caution should be exercised*, especially when dealing with the unsolvated form because of its thermal and shock sensitivity. Literature procedures were employed and modified for the preparation of the following complexes: $(CGC)MCl_2$ (M = Ti, Zr),[64h] $(CGC)TiMe_2$,[64h,68] and $(CGC)TiMe^+MeB(C_6F_5)_3^-$ (**1**).[69]

Preparation of Lithium Isopropyl Isobutyrate, $Me_2C{=}C(O^iPr)OLi$. A literature procedure[70] for the general synthesis of unsolvated ketone and ester enolates using the in situ generated lithium diisopropylamide (LDA) in hexanes was modified for the preparation of $Me_2C{=}C(O^iPr)OLi$. In an argon-filled glovebox, a 200 mL Schlenk flask was equipped with a magnetic stir bar and charged with 50 mL of hexanes. This flask was sealed with a rubber septum, removed from the glovebox, interfaced to a Schlenk line, and placed in a 0 °C ice−water bath. Diisopropylamine (6.63 g, 65.6 mmol, predried) was added to this flask via syringe, followed by addition of ^{n}BuLi (42 mL, 1.6 M in hexanes, 67.2 mmol) dropwise via a syringe. The mixture was stirred for 30 min at 0 °C to generate LDA in situ, after which isopropyl isobutyrate (10 mL, 8.47 g, 65.1 mmol, predried) was added via syringe. The reaction mixture was warmed gradually to room temperature and stirred for another 2 h. All volatiles were removed in vacuo, and the residue was thoroughly dried in vacuo to give 8.1 g (91%) of the spectroscopically pure product as a white powder. When needed, further purification can be carried out by recrystallization from hexanes at −30 °C to give colorless crystals. ^{1}H NMR (C_6D_6, 23 °C): δ 4.28 (sept, 1H, −OC*H*Me$_2$), 1.86 (s, 3H, =C*Me*$_2$), 1.76 (s, 3H, =C*Me*$_2$), 1.24 (d, 6H, −CH*Me*$_2$). ^{13}C NMR (C_6D_6, 23 °C): δ

156.2 [*C*═O(O*i*Pr)], 78.01 (═*C*Me$_2$), 72.21 (O*C*HMe$_2$), 22.27 (OCH*Me*$_2$), 18.07 (═C*Me*$_2$), 17.71 (═C*Me*$_2$). We have previously characterized the molecular structure of the unsolvated Me$_2$C═C(O*i*Pr)OLi by single-crystal X-ray diffraction analysis.[71]

Synthesis of (CGC)Ti[OC(O*i*Pr)═CMe$_2$]$_2$ (4). This synthesis consists of the following three steps involving the use of the intermediates (CGC)TiMe$_2$ and (CGC)Ti(OTf)$_2$. First, in a nitrogen-filled glovebox, a 250 mL glass reactor was equipped with a magnetic stir bar, charged with (CGC)TiCl$_2$ (1.00 g, 2.72 mmol) and 80 mL of Et$_2$O, and subsequently cooled to −30 °C inside the glovebox freezer. A solution of MeMgBr (2.0 mL, 3.0 M in diethyl ether, 6.0 mmol) was added via syringe to the above prechilled, vigorously stirred reactor. The resulting green-yellow mixture was stirred overnight at ambient temperature, after which all volatiles were removed under reduced pressure. The pure (CGC)TiMe$_2$ as a yellow-green solid was obtained after sublimation at ca. 75 °C on a high-vacuum line for ≥6 h, and the yield was 0.65 g (73%). ^{1}H NMR (CD$_2$Cl$_2$, 23 °C) for (CGC)TiMe$_2$: δ 2.14 (s, 6H, C$_5$*Me*$_4$), 1.88 (s, 6H, C$_5$*Me*$_4$), 1.54 (s, 9H, NC*Me*$_3$), 0.45 (s, 6H, Ti*Me*$_2$), 0.13 (s, 6H, Si*Me*$_2$). ^{1}H NMR (C$_6$D$_6$, 23 °C) for CGCTiMe$_2$: δ 1.96 (s, 6H, C$_5$*Me*$_4$), 1.85 (s, 6H, C$_5$*Me*$_4$), 1.57 (s, 9H, NC*Me*$_3$), 0.51 (s, 6H, Ti*Me*$_2$), 0.43 (s, 6H, Si*Me*$_2$).

Next, in an argon-filled glovebox, a 50 mL Schlenk flask was equipped with a stir bar and charged with 30 mL of toluene and 0.27 g (0.82 mmol) of (CGC)TiMe$_2$. The flask was sealed with a rubber septum, removed from the glovebox, and interfaced to a Schlenk line. The yellow solution was cooled to −78 °C, and to this solution was quickly added triflic acid (0.15 mL, 0.25 g, 1.7 mmol) via a glass syringe. The flask was warmed gradually to room temperature over 1 h, and the resulting dark red mixture was stirred overnight. The flask was taken into the glovebox after all volatiles were removed in vacuo. The solid residue was extracted with toluene until colorless, and the extract was filtered through a pad of Celite. The dark red filtrate was concentrated and left inside a −30 °C freezer overnight, yielding 0.13 g (27%) of the pure product (CGC)Ti(OTf)$_2$ as red needle-like crystals. ^{1}H NMR (CD$_2$Cl$_2$, 23 °C) for (CGC)Ti(OTf)$_2$: δ 1.94 (s, 6H, C$_5$*Me*$_4$), 1.88 (s, 6H, C$_5$*Me*$_4$), 1.13 (s, 9H, NC*Me*$_3$), 0.28 (s, 6H, Si*Me*$_2$). ^{19}F NMR (CD$_2$Cl$_2$, 23 °C): δ −156.85 (s).

Third, in a nitrogen-filled glovebox, a 30 mL glass reactor was equipped with a magnetic stir bar, charged with 15 mL of toluene, and cooled to −30 °C inside a glovebox freezer. To this prechilled reactor, with vigorous stirring, was added (CGC)Ti(OTf)$_2$ (35.4 mg, 0.060 mmol) followed by addition of lithium isopropyl isobutyrate (23.0 mg, 0.17 mmol). The resulting suspension was stirred overnight at ambient temperature, after which it was filtered through a pad of Celite. The solvent of the filtrate was removed in vacuo, yielding 28.0 mg (85%) of the spectroscopically pure final product **4** as a red oily product which can be crystallized at low temperatures, but the obtained crystals melt immediately on warming to ambient temperature. The isolated complex is somewhat unstable at ambient temperature for an extended time period (several hours), thus not suitable for shipping out for elemental analysis, but it can be readily characterized by NMR. ^{1}H NMR (C$_6$D$_6$, 23 °C) for (CGC)Ti[OC(O*i*Pr)═CMe$_2$]$_2$ (**4**): δ 4.41 (sept, J = 6.3 Hz, 2H, C*H*Me$_2$), 2.23 (s, 6H, C$_5$*Me*$_4$), 1.99 (s, 6H, C$_5$*Me*$_4$), 1.84 (s, 6H, ═C*Me*$_2$), 1.83 (s, 6H, ═C*Me*$_2$), 1.38 (s, 9H, NC*Me*$_3$), 1.20 (d, J = 6.3 Hz, 6H, CH*Me*$_2$), 1.18 (d, J = 6.3 Hz, 6H, CH*Me*$_2$), 0.63 (s, 6H, Si*Me*$_2$). ^{13}C NMR (C$_6$D$_6$, 23 °C): δ 156.8 [*C*(O*i*Pr)═O], 133.6 (*C*$_5$Me$_4$), 132.7 (*C*$_5$Me$_4$), 105.4 (*C*$_5$Me$_4$), 90.03 (═*C*Me), 69.20 (*C*HMe$_2$), 59.40 (*C*Me$_3$), 33.61 (C*Me*$_3$), 22.50 (CH*Me*$_2$), 22.23 (CH*Me*$_2$), 19.52 (═C*Me*), 18.48 (═C*Me*), 14.69 (C$_5$*Me*$_4$), 11.16 (C$_5$*Me*$_4$), 7.08 (Si*Me*$_2$).

Synthesis of (CGC)Zr[OC(O*i*Pr)═CMe$_2$]$_2$ (5). The same approach for the synthesis of analogous (CGC)Zr[OC(O*t*Bu)═CMe$_2$]$_2$[34] was utilized for the synthesis of **3** with a detailed and modified procedure given below. In a nitrogen-filled glovebox, a 100 mL Schlenk flask was equipped with a magnetic stir bar and charged with (CGC)ZrCl$_2$ (0.50 g, 1.2 mmol) and 20 mL of THF. The flask was sealed with a rubber septum, interfaced to a Schlenk line, and suspended in a dry ice−acetone bath at −78 °C. A solution of Me$_2$C═C(O*i*Pr)OLi (0.34 g, 2.5 mmol) in 20 mL of THF contained in a Schlenk flask was added to the above stirred solution via a cannular. The resulting mixture was allowed to warm gradually to ambient temperature and stirred overnight, after which all volatiles were removed in vacuo to give a light yellow solid. The flask was brought back into the glovebox, and the solid was extracted with 40 mL of hexanes. The extract was filtered through a pad of Celite, and the filtrate was dried in vacuo to give 0.68 g (93%) of the crude product as a light yellow oil. The oil was dissolved in 2−3 mL of hexanes and cooled to −30 °C. Precipitates (impurities) formed were removed by filtration, and the solvent of the filtrate was removed to give 0.49 g (67%) of the spectroscopically pure product **3** as a yellow solid. ^{1}H NMR (C$_6$D$_6$, 23 °C) for (CGC)Zr[OC(O*i*Pr)═CMe$_2$]$_2$ (**5**): δ 4.41 (sept, J = 6.3 Hz, 2H, C*H*Me$_2$), 2.22 (s, 6H, C$_5$*Me*$_4$), 2.00 (s, 6H, C$_5$*Me*$_4$), 1.84 (s, 6H, ═C*Me*$_2$), 1.80 (s, 6H, ═C*Me*$_2$), 1.34 (s, 9H, NC*Me*$_3$), 1.19 (d, J = 6.3 Hz, 12H, CH*Me*$_2$), 0.62 (s, 6H, Si*Me*$_2$).

Isolation of Active Species (CGC)Zr$^+$[OC(O*i*Pr)═C(Me)-CH$_2$C(Me$_2$)C(O*i*Pr)═O][B(C$_6$F$_5$)$_4$]$^-$ (6). In an argon-filled glovebox, a 4 mL glass vial was charged with complex **3** (12.0 mg, 0.020 mmol) and 0.4 mL of CH$_2$Cl$_2$, while another vial was charged with [Ph$_3$C][B(C$_6$F$_5$)$_4$] (18.4 mg, 0.020 mmol) and 0.4 mL of CH$_2$Cl$_2$. The two vials were mixed via a pipet at ambient temperature to give instantaneously a yellow-green solution. The solvent was removed in vacuo, and the residue was washed with 5 mL of hexanes to give a yellow-green oily product; subsequent analysis by NMR showed the clean and quantitative formation of ion pair **6**. Anal. Calcd for C$_{53}$H$_{52}$BO$_4$F$_{20}$NSiZr: C, 49.84; H, 4.11. Found: C, 49.57; H, 4.63. ^{1}H NMR (CD$_2$Cl$_2$, 23 °C) for **6**: δ 5.24 (sept, J = 6.0 Hz, 1H, C*H*Me$_2$), 4.30 (sept, J = 6.3 Hz, 1H, C*H*Me$_2$), 2.24 (s, 3H, C$_5$*Me*$_4$), 2.22 (s, 3H, C$_5$*Me*$_4$), 2.11 (s, 3H, C$_5$*Me*$_4$), 1.99 (s, 3H, C$_5$*Me*$_4$), 1.63 (s, br, 2H, C*H*$_2$), 1.47 (d, J = 6.0 Hz, 3H, CH*Me*$_2$), 1.43 (d, J = 6.0 Hz, 3H, CH*Me*$_2$), 1.42 (s, 3H, ═C*Me*), 1.34 (s, 3H, C*Me*$_2$), 1.28 (d, J = 6.3 Hz, 3H, CH*Me*$_2$), 1.27 (s, 3H, C*Me*$_2$), 1.22 (d, J = 6.3 Hz, 3H, CH*Me*$_2$), 1.17 (s, 9H, NC*Me*$_3$), 0.73 (s, 3H, Si*Me*$_2$), 0.66 (s, 3H, Si*Me*$_2$). ^{19}F NMR (CD$_2$Cl$_2$, 23 °C): δ −131.5 (d, $^3J_{F-F}$ = 13.6 Hz, 8F, *o*-F), −162.0 (t, $^3J_{F-F}$ = 22.2 Hz, 4F, *p*-F), −165.9 (m, 8F, *m*-F).

In Situ Generation of (CGC)Zr[OC(O*i*Pr)═CMe$_2$]$^+$[O═C(O*i*Pr)CMe$_2$B(C$_6$F$_5$)$_3$]$^-$ (7). In an argon-filled glovebox, a 4 mL glass vial was charged with complex **3** (12.0 mg, 0.020 mmol) and 0.4 mL of CD$_2$Cl$_2$, while another vial was charged with B(C$_6$F$_5$)$_3$ (10.2 mg, 0.020 mmol) and 0.4 mL of CD$_2$Cl$_2$. The two vials were mixed via pipet at ambient temperature to give instantaneously a red solution; subsequent analysis of this red solution by NMR showed the clean and quantitative formation of ion pair **5**. The isolated complex is somewhat unstable at ambient temperature for an extended time period (several hours), thus not suitable for shipping out for elemental analysis. ^{1}H NMR (CD$_2$Cl$_2$, 23 °C) for **7**: δ 5.24 (sept, J = 6.3 Hz, 1H, C*H*Me$_2$), 4.30 (sept, J = 6.0 Hz, 1H, C*H*Me$_2$), 2.23 (s, 3H, C$_5$*Me*$_4$), 2.22 (s, 3H, C$_5$*Me*$_4$), 2.10 (s, 3H, C$_5$*Me*$_4$), 1.99 (s, 3H, C$_5$*Me*$_4$), 1.62 (s, 3H, ═C*Me*$_2$), 1.47 (d, J = 6.0 Hz, 6H, CH*Me*$_2$), 1.41 (s, 3H, ═C*Me*$_2$), 1.34 (s, 3H, C*Me*$_2$), 1.29 (s, 3H, C*Me*$_2$), 1.23 (d, J = 6.3 Hz, 6H, CH*Me*$_2$), 1.17 (s, 9H, NC*Me*$_3$), 0.73 (s, 3H, Si*Me*$_2$), 0.66 (s, 3H, Si*Me*$_2$). ^{19}F NMR (CD$_2$Cl$_2$, 23 °C): δ −132.3 (br, 6F, *o*-F), −163.2 (br, 3F, *p*-F), −165.9 (br, 6F, *m*-F).

General Polymerization Procedures. Polymerizations were performed either in 25 mL flame-dried Schlenk flasks interfaced to the dual-manifold Schlenk line for runs using an external temperature bath or in 30 mL glass reactors inside the glovebox for ambient temperature (ca. 25 °C) runs. Catalyst precursors (CGC)TiMe$_2$, (CGC)Ti[OC(O*i*Pr)═CMe$_2$]$_2$, and (CGC)Zr[OC(O*i*Pr)═CMe$_2$]$_2$ were premixed with an equimolar amount of an appropriate activator B(C$_6$F$_5$)$_3$, Al(C$_6$F$_5$)$_3$, [Ph$_3$C][B(C$_6$F$_5$)$_4$], or [HNMe$_2$Ph][B(C$_6$F$_5$)$_4$] as indicated, in a toluene or CH$_2$Cl$_2$ solution for ca. 30 min [when activated with B(C$_6$F$_5$)$_3$] or 10 min (for all other activators) to generate the corresponding activated species. The polymerization was started by rapid addition of MMA (typically 1.00 mL, 9.35 mmol, or a different amount according to the [MMA]$_0$/[(CGC)M]$_0$ ratio specified in the text) under vigorous

stirring at the pre-equilibrated bath temperature. After the measured time interval, a 0.2 mL aliquot was taken from the reaction mixture via a syringe and quickly quenched into a 4 mL vial containing 0.6 mL of undried "wet" $CDCl_3$ stabilized by 250 ppm of BHT-H; the quenched aliquots were analyzed by ^{1}H NMR to obtain the percent monomer conversion data. The polymerization was immediately quenched after the removal of the aliquot by addition of 5 mL 5% HCl-acidified methanol. The quenched mixture was precipitated into 100 mL of methanol, stirred for 1 h, filtered, washed with methanol, and dried in a vacuum oven at 50 °C overnight to a constant weight.

Polymerization Kinetics. Kinetic experiments (conditions: $[MMA]_0/[\mathbf{1}]_0 = 200$, 9.35 mmol of MMA, 46.8 μmol of (CGC)-$TiMe_2$ and $B(C_6F_5)_3$, 10 mL of CH_2Cl_2 or toluene, ca. 25 °C) were carried out in a stirred glass reactor inside the glovebox. The procedures for obtaining the monomer conversion vs reaction time data were described in literature.[9,71] Specifically, at appropriate time intervals, 0.2 mL aliquots were withdrawn from the reaction mixture using a syringe and quickly quenched into 1 mL vials containing 0.6 mL of undried "wet" $CDCl_3$ mixed with 250 ppm of BHT-H. The quenched aliquots were analyzed by ^{1}H NMR. The ratio of $[MMA]_0$ to $[MMA]_t$ at a given time t, $[MMA]_0/[MMA]_t$, was determined by integration of the peaks for MMA (5.2 and 6.1 ppm for the vinyl signals; 3.4 ppm for the O*Me* signal) and PMMA (centered at 3.4 ppm for the O*Me* signals) according to $[MMA]_0/[MMA]_t = 2A_{3.4}/3A_{5.2+6.1}$, where $A_{3.4}$ is the total integrals for the peaks centered at 3.4 ppm (typically in the region 3.2−3.6 ppm) and $A_{5.2+6.1}$ is the total integrals for both peaks at 5.2 and 6.1 ppm. The obtained conversion vs time date were plotted in two ways: $[MMA]_t/[MMA]_0$ vs time plot for the zero-order kinetics in [MMA] or $\ln([MMA]_0/[MMA]_t)$ vs time plot for the first-order kinetics in [MMA]. The best linearly fit plots were used to determine the kinetic order, and the apparent rate constant (k_{app}) for each run were obtained from the slope of the best-fit line.

Polymer Characterizations. Polymer number-average molecular weights (M_n) and molecular weight distributions (PDI = M_w/M_n) were measured by gel permeation chromatography (GPC) analyses carried out at 40 °C and a flow rate of 1.0 mL/min, with THF as the eluent on a Waters University 1500 GPC instrument equipped with one PLgel 5 μm guard and three PLgel 5 μm mixed-C columns (Polymer Laboratories; linear range of molecular weight = 200−2 000 000). The instrument was calibrated with 10 PMMA standards, and chromatograms were processed with Waters Empower software (version 2002). ^{1}H NMR spectra for the analysis of PMMA microstructures were recorded in $CDCl_3$ and analyzed according to the literature methods.[13,18,72]

Models and Computational Details. The Amsterdam Density Functional (ADF) program was used to obtain all the results concerned with the mechanism of stereoselectivity.[73] The electronic configuration of the molecular systems was described by a triple-ζ STO basis set on Ti and Zr (ADF basis set TZV).[73a] Triple-ζ STO basis sets, augmented by one polarization function, were used for main group atoms (ADF basis sets TZVP).[73a] The inner shells on Ti and Zr (including 2p and 3d, respectively), Si (including 2p), C, N, and O (1s) were treated within the frozen core approximation. Energies and geometries were evaluated using the local exchange-correlation potential by Vosko et al.,[74] augmented in a self-consistent manner with Becke's[75] exchange gradient correction and Perdew's[76] correlation gradient correction (BP86 functional). All geometries were localized in the gas phase. However, since MMA polymerization is usually performed in a rather polar solvent, such as CH_2Cl_2, we performed single point energy calculations on the final geometries to take into account solvent effects. The ADF implementation of the conductor-like screening model (COSMO)[77] was used. A dielectric constant of 8.9 and a solvent radius of 2.94 Å were used to represent CH_2Cl_2 as the solvent. The following radii, in angstroms, were used for the atoms: H 1.16, C 2.00, N 1.40, O 1.50, Si 2.20, Ti 2.30, and Zr 2.40. All the reported energies include solvent effects.

The Turbomole (TM) package[78] was used to obtain all the results concerned with the mechanism of site epimerization. The electronic configuration of the molecular systems was described by a triple-ζ basis set on Ti (TM basis set def-TZVP).[79] A double-ζ basis set, augmented by one polarization function, was used for main group atoms (TM basis sets def-SVP).[79] Core electrons of Zr (up to 3d) were treated with the Stuttgart−Dresden pseudopotential.[80] Energies and geometries were evaluated with the BP86 functional. Solvent effects (both CH_2Cl_2 and toluene, with a dielectric constant of 8.9 and 2.38, respectively) were evaluated with the COSMO model through single point energy calculations on the final gas-phase geometries. The following radii, in angstroms, were used for the atoms: H 1.404, C 1.989, N 1.813, O 1.778, Si 2.457, and Ti 2.223. All the reported energies include solvent effects.

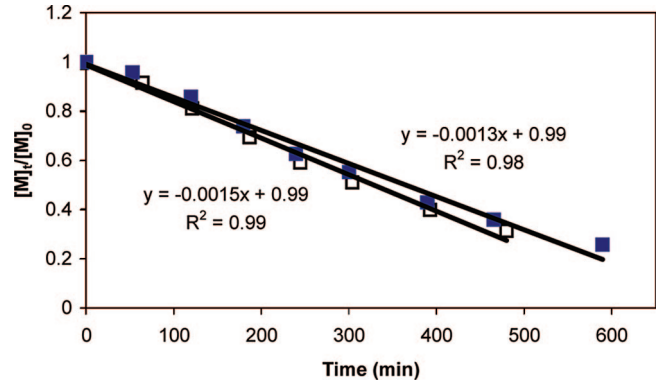

Figure 1. Zero-order plots of $[MMA]_t/[MMA]_0$ vs time for the polymerization of MMA by **1** in toluene (■) and CH_2Cl_2 (□) at 25 °C. Conditions: 9.35 mmol of MMA, 46.8 μmol of (CGC)$TiMe_2$ and $B(C_6F_5)_3$ in 10 mL of a solvent for a $[MMA]_0/[\mathbf{1}]_0$ ratio of 200.

Results and Discussion

Kinetics of Polymerization by the (CGC)Ti Catalyst. MMA polymerization by the cationic alkyl complex **1** was detailed in several publications.[6,18,28] The living and high-efficiency polymerization by the thermally stable alkyl complex **1** implies that k_i (rate of initiation) by the Ti−*Me* ligand is $\geq k_p$ (rate of propagation) by the Ti−*ester enolate* ligand, derived from the initiation step involving nucleophilic attack of the Ti methyl group at the MMA coordinated to the cationic Ti center, and that this polymerization is largely devoid of chain termination or transfer side reactions. This feature renders **1** ideal for investigation of its polymerization kinetics. However, there is no report on such a study, and consequently a fundamental question of whether this polymerization by the C_s-ligated complex **1** follows the same kinetics as that by the C_2-ligated unimetallic complex,[9] or not, remained unaddressed. This information is also needed for elucidating the mechanisms of the polymerization and stereocontrol (vide infra). To this end, we set out to examine the kinetics of the MMA polymerization by **1**, the results of which were summarized in Figure 1.

Intriguingly, the MMA polymerization by **1** in either toluene or CH_2Cl_2 follows zero-order kinetics with respect to MMA concentration (Figure 1). This result is in sharp contrast to the first-order kinetics observed for the *ansa*-C_2-ligated catalyst in which propagation "catalysis" cycle intramolecular conjugate Michael addition in catalyst−monomer complex **A** leading to the eight-membered-ring cyclic ester enolate chelate (resting active intermediate **B**) is *fast* relative to associative displacement of the coordinated ester group in **B** by the incoming monomer (i.e., the rate-limiting ring-opening of the chelate) to regenerate **A** (Scheme 2).[9] Conversely, the zero-order kinetics in [MMA] observed for the (CGC)Ti catalyst **1** suggests a different scenario: Michael addition in catalyst−monomer complex **A′** leading to the cyclic chelate **B′** is *slow* relative to associative displacement of the coordinated ester group in **B′** by the incoming monomer (Scheme 2). The observed similar rates of

Scheme 2

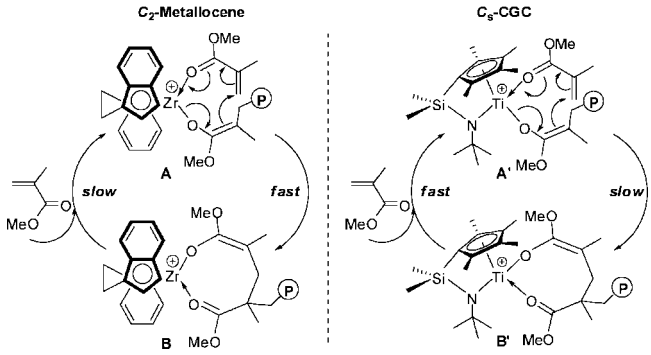

Table 1. Selected MMA Polymerization Results by (CGC)TiMe$^+$MeB(C$_6$F$_5$)$_3^-$ (1)^a

run no.	[1] (mM)	[MMA] (M)	[MMA]$_0$/[1]$_0$	[*rr*]^b (%)	[*mr*]^b (%)	[*mm*]^b (%)
1	4.67	1.87	400	78	19	3
2	4.67	0.935	200	79	19	2
3	4.67	0.467	100	79	19	2
4	4.67	0.234	50	76	21	3
5	1.17	0.467	400	79	19	2

^{a} Carried out in an argon-filled glovebox at ambient temperature (~25 °C) in CH_2Cl_2 for 12 h. ^{b} Tacticity measured by ^{1}H NMR.

polymerization (k_{app} = 1.3 × 10^{-3} mol/L s^{-1} in toluene and 1.5 × 10^{-3} mol/L s^{-1} in CH_2Cl_2, Figure 1) are consistent with the MMA addition being the rate-determining step. This unique observation for the unimetallic MMA propagation system **1**[18] that exhibits a relatively faster ring-opening process provides a kinetic basis for feasible pathways leading to MMA- or anion-assisted epimerization at Ti before MMA additions (vide infra).

Effects of Monomer and Catalyst Concentrations, Anion Structure, and Solvent Polarity on Syndioselectivity. To ascertain whether the monomer concentration would affect the resulting PMMA syndiotacticity, we kept [**1**]$_0$ constant (4.67 mM in toluene) and varied [MMA]$_0$ by 12-fold (i.e., from 2.81 to 0.234 M). The polymerizations were carried out at T_p of 25 °C for 12 h, achieving high MMA conversions (93−99%) for all of the [MMA]$_0$/[**1**]$_0$ ratios employed. Interestingly, the syndiotacticity [*rr*] was kept within a 77%−74% range over a 12-fold [MMA] change and is thus largely [MMA]-invariant considering typical errors associated with the tacticity measurement being ≤2%. The *mr* (in a 19%−22% range) and *mm* (in a 3%−4% range) stereoerrors are also insensitive to monomer concentration. Likewise, the same polymerization carried out in CH_2Cl_2 gave similar results (runs 1−4, Table 1). Lastly, a 4-fold reduction of the catalyst concentration while keeping [MMA] the same yielded identical tacticities (run 5 vs run 3). Overall, the syndiotacticity of the C_s-ligated (CGC)Ti catalyst **1** is insensitive to both concentrations of monomer and catalyst as well as to solvent polarity (more on this point is described below), and the resulting syndiotactic PMMA contains predominately isolated *m* stereoerrors. This observation can be explained by a scenario in which the syndioselectivity of the polymerization is regulated by the chiral catalyst site and catalyst site epimerization after a stereomistake is responsible for the isolated *m* stereoerrors (vide infra).

Next, we examined potential effects of ion-pairing strength, varied with anion structure and solvent polarity, on the syndioselectivity of the polymerization by the (CGC)Ti catalyst. Under identical conditions (9.35 mmol of MMA, 46.8 μmol of (CGC)TiMe$_2$ and activator, [MMA]$_0$/[Ti]$_0$ = 200, 10 mL of toluene, 25 °C), the catalyst systems derived from activation of (CGC)TiMe$_2$ with B(C$_6$F$_5$)$_3$, [Ph$_3$C][B(C$_6$F$_5$)$_4$], and [HNMe$_2$Ph][B(C$_6$F$_5$)$_4$] gave syndiotactic PMMA with the syndiotacticity kept within a 77% *rr*−80% *rr* range, showing negligible anion effect. Additionally, for all of the above three systems investigated there is no noticeable syndiotacticity change (<2% *rr*) by switching the solvent from toluene to polar, essentially noncoordinating CH_2Cl_2. In short, these results indicate that, *in marked contrast* to the propylene polymerization by C_s-symmetric metallocene catalysts,[81] ion-pairing has little to negligible effects on the syndioselectivity of the MMA polymerization by the C_s-symmetric (CGC)Ti catalyst.

Effects of Metal (Zr vs Ti) on Syndioselectivity. Unlike the (CGC)Ti complex **1**, the isostructural Zr alkyl complex (CGC)ZrMe$^+$MeB(C$_6$F$_5$)$_3^-$ is inactive for the polymerization of MMA, prohibiting us from making a direct comparison using these (CGC)M alkyl complexes. Accordingly, we set out the synthesis of their identical bis(ester enolate) complexes **4** and **5** (Scheme 3) because the cationic (CGC)Zr *tert*-butyl ester enolate complex **3** has been shown to be active for MMA polymerization at low T_p.[34]

We elected to synthesize their *isopropyl* isobutyrate complexes because neutral metallocene *methyl* isobutyrate complexes and cationic *tert-butyl* isobutyrate complexes are not stable at room temperature due to ketene formation and isobutylene elimination,[19,34] respectively, whereas both neutral and cationic metallocene *isopropyl* isobutyrate complexes are stable at room temperature.[13] Indeed, both neutral (CGC)Ti and Zr bis(isopropyl ester enolate) complexes **4** and **5** as well as the cationic ester enolate (CGC)Zr complex **6** were successfully isolated (Scheme 3 and Experimental Section). The (CGC)Zr bis(ester enolate) complex **5** was obtained in a straightforward fashion, that is, one-step reaction of (CGC)ZrCl$_2$ with Me$_2$C═C(O^{i}Pr)OLi. The same route failed to give the isostructural (CGC)Ti bis(ester enolate) complex **4**; however, its synthesis was accomplished by a three-step route: methylation of (CGC)TiCl$_2$ to give (CGC)TiMe$_2$, protonolysis with triflic acid to yield (CGC)Ti(OTf)$_2$, and nucleophilic ligand substitution with Me$_2$C═C(O^{i}Pr)OLi to afford **4**. The cationic (CGC)Zr ester enolate complex **6** was generated by oxidative activation of **5** using [Ph$_3$C][B(C$_6$F$_5$)$_4$] via a pathway that has already been demonstrated for another C_s-ligated zirconocene bis(ester enolate) catalyst precursor with a different ligand framework;[4] the entire activation process involves hydride abstraction from the methyl group within the enolate [OC(O^{i}Pr)═CMe$_2$] moiety by [Ph$_3$C]$^+$, followed by nucleophilic addition of another enolate ligand to the resulting isopropyl methacrylate coordinated to the metal center, finally affording the cationic eight-membered-ring active species **6**.

Results of the MMA polymerization at ambient temperature by the bis(ester enolate) complexes **4** and **5** activated with three different types of activators are summarized in Table 2. The B(C$_6$F$_5$)$_3$ activation of the Zr complex **5** generates the tight ion-pairing complex **7**, which exhibits low activity, but nonetheless affords syndiotactic PMMA at 25 °C (70% *rr*, PDI = 1.15, run 1). Addition of another equivalent of B(C$_6$F$_5$)$_3$ slightly increased MMA conversion from 20% to 26% but left the syndiotacticity and PDI values unchanged (runs 2 vs 1); this experiment ruled out the possible bimetallic pathway contributing to the observed syndiotacticity (the *rr* is 64% when 0.5 equiv of B(C$_6$F$_5$)$_3$ relative to **5** or Cp$_2$Zr[OC(O^{i}Pr)═CMe$_2$]$_2$ was used for the bimetallic system). Similar B(C$_6$F$_5$)$_3$ activation products of C_2- and C_{2v}-ligated Zr analogues and their polymerization characteristics have been observed previously.[7,82] On the other hand, the **5** + 2Al(C$_6$F$_5$)$_3$ system gave quantitative MMA conversion, while the **5** + Al(C$_6$F$_5$)$_3$ system achieved only 66% under the same conditions, although the syndiotacticity (72% *rr*) of the resulting PMMA is identical (runs 4 vs 3); this observation can be attributed to the propagation onto the enolaluminate intermediate for the metallocene + Al(C$_6$F$_5$)$_3$ system.[7,23,32,82]

Scheme 3

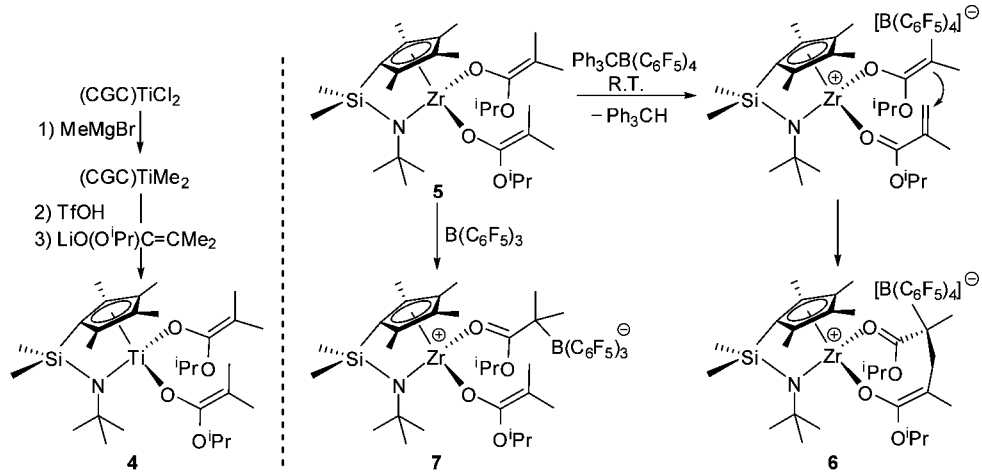

Table 2. Selected MMA Polymerization Results by (CGC)M[bis(ester enolate)] Complexes 4 and 5[a]

run no.	metal (mM)	activator (*x* equiv)	[MMA]/[metal]	solvent[b]	temp (°C)	time (h)	conv (%)	[*rr*] (%)
1	**5** (2.13)	$B(C_6F_5)_3$	400	DCM	25	21	20	70
2	**5** (2.13)	$B(C_6F_5)_3$ (2)	400	DCM	25	21	26	70
3	**5** (2.13)	$Al(C_6F_5)_3$	400	DCM	25	3	66	72
4	**5** (2.13)	$Al(C_6F_5)_3$ (2)	400	DCM	25	3	100	72
5	**5** (38)	$[HNMe_2Ph][B(C_6F_5)_4]$	187.5	DCM + T	25	24	67	43
6	**4** (38)	$[HNMe_2Ph][B(C_6F_5)_4]$	187.5	DCM + T	25	24	100	74

[a] Monomer conversion (%) and syndiotacticity (% *rr*) determined by ^1H NMR; $T_p = \sim 25$ °C. [b] 10 mL of dichloromethane (DCM) when DCM used alone or 0.25 mL of DCM (activator solution) plus 0.25 mL of T (toluene solution of the metal complex) when DCM and T mixed together (DCM + T).

Scheme 4

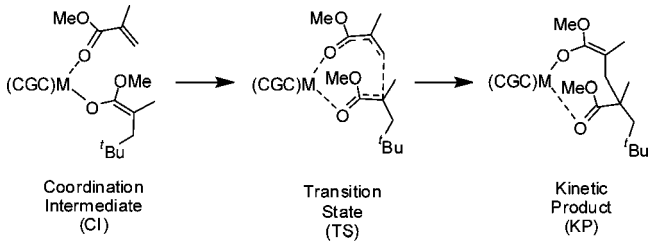

The MMA polymerization of **5** activated with the protonolysis activator $[HNMe_2Ph][B(C_6F_5)_4]$, an increased catalyst concentration, and the use of a CH_2Cl_2/toluene mixture produced syndio-enriched atactic PMMA (43% *rr*, run 5). Switching to the (CGC)Ti complex **4** with the same $[HNMe_2Ph][B(C_6F_5)_4]$ activator significantly increased the PMMA syndiotacticity to 74% *rr* (run 6). The above results show that both (CGC)Ti and Zr isopropyl ester enolate catalyst systems derived from the activators currently employed are syndioselective at ambient temperature, and the (CGC)Ti system exhibits higher syndioselectivity.

Computational Insights into the Mechanism of MMA Polymerization. In this section we provide a computational rationalization of the chemical scenario resulting from the experiments. Specifically, we focused on the Michael addition step (Scheme 4). Since the experimental results indicate that the counterion has negligible effects on the syndioselectivity of the polymerization, the models we used to investigate the chain growth step did not include the counterion, and we started from the coordination intermediate (CI). The reaction follows with MMA addition through the transition state (TS) for the Michael addition and collapses to a species we called the kinetic product (KP). We calculated these steps for both Ti and Zr systems and considered the two enantiofaces of the ester enolate growing chain, which means we focused on the enantioselectivity of the MMA addition. In all cases we considered an *S* chirality at the metal. Finally, on the basis of our previous theoretical results, we only focused on transition states presenting a relative *trans* disposition of the methoxy groups of both the growing chain and the monomer.[56,57]

As shown in Figure 2, for both the Ti and Zr systems the *re*-face of the enolate growing chain reacts preferentially in the case of an *S*-chirality at the metal. In both systems there is a selection of the *re*-face of the chain even at the coordination intermediate, although enantioselectivity is determined by the energy difference at the transition state. Within this framework the ΔE_{stereo} is 2.3 and 1.9 kcal/mol for the Ti and Zr systems, respectively. This result means that both systems are enantioselective, although the Ti system is somewhat more enantioselective than the Zr analogue, which is in qualitative agreement with our experimental findings. Finally, there is a non-negligible energy difference also in the kinetic products that correspond to the eight-membered cycles that are obtained

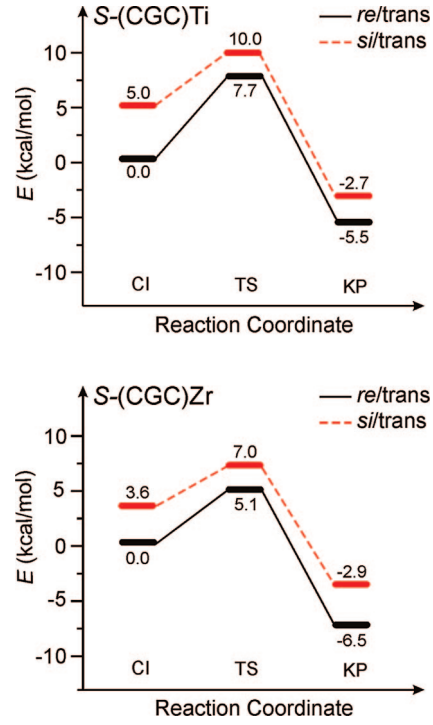

Figure 2. Energy diagrams for MMA addition to the *S*-metal center (energies in kcal/mol).

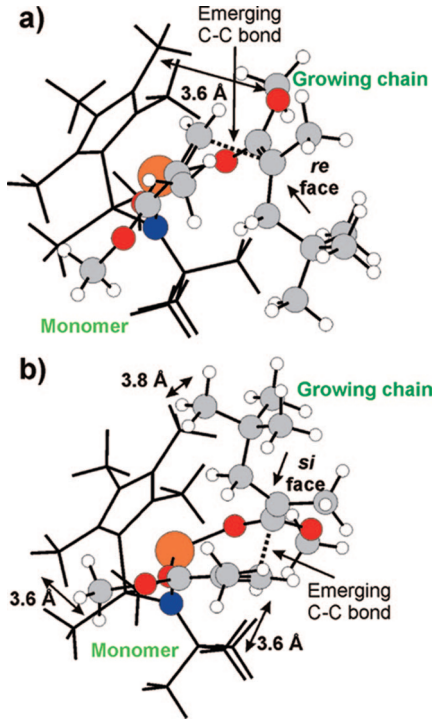

Figure 3. Transition states for MMA addition with the (CGC)Ti system with an *S*-configuration at the Ti atom. Atoms depicted in spheres are Ti in orange, O in red, N in blue, C in gray, and H in white.

from collapsing the two transition states on the products side. The exothermicity of the chain growth step from the coordination intermediate to the products is ~5 kcal/mol, which is remarkably smaller than that of ethene or propene polymerization (~20 kcal/mol).[83]

The geometries of the two competing transition states of the (CGC)Ti system are shown in Figure 3. It is clear that the opposite enantiofaces of the enolate chain result in rather different orientation of the growing chain with respect to the bulky Cp′ (η^5-Me_4C_5) ligand. In the favored transition state (*re*-chain with an *S*-metal) the bulky ^{t}Bu group of the growing chain is oriented toward the N-group and away from the Cp′ ligand, whereas in the unfavored transition state (*si*-chain with an *S*-metal) the bulky ^{t}Bu group of the growing chain sterically interacts with the Cp′ ligand. This steric interaction is more relevant at the level of eight-membered products, when the new C−C bond is completely formed and the back-bonding of the chain pulls the ^{t}Bu group in close proximity of the Cp′ ligand.

The eight-membered product corresponding to the favored transition state (*S*-metal/*re*-chain) is 2.8 and 3.6 kcal/mol lower in energy than the product corresponding to a stereomistake (*S*-metal/*si*-chain) for the Ti and Zr systems, respectively. This result suggests that there might be a rearrangement of the kinetic product corresponding to the stereomistake toward a more stable resting state. This rearrangement involves a site epimerization reaction, as shown in Scheme 5. Owing to this site epimerization reaction, the higher energy kinetic product corresponding to a steromistake (*S*-metal/*si*-chain) evolves into the *R*-metal/*si*-chain resting state that, by symmetry, is isoenergetic with the thermodynamic *S*-metal/*re*-chain product that is obtained from the favored transition state. To check whether this site epimerization reaction is possible, we started to break the back-bonding of the last C═O (ester) unit. However, in the gas phase or even in the presence of solvent effects dissociation of the last C═O unit from the metal is energetically quite difficult. For this reason, we used two different models: site epimerization assisted by an additional MMA molecule or by an explicit $MeB(C_6F_5)_3^-$ counterion. As shown in Scheme 5, two possible pathways can be envisaged: one that involves a back-side attack of the counterion or the monomer and the other that involves a front-side attack. Owing to the extreme flexibility of this species, we believe that a detailed investigation of the preferred pathway is almost infeasible without using a molecular dynamics approach, and it is not a case that even in the much more thoroughly investigated propene polymerization a theoretical description of the counterion assisted site epimerization has been proposed only 1 year ago.[84] For this reason, we only focused on the intermediates along one of the two pathways, specifically the front-side pathway, in order to explore its energetic feasibility.

The energetics associated with the mechanism depicted in Scheme 5 is reported in Figure 4. First, in the presence of a MMA molecule or a counterion, the *S*-metal/*si*-chain kinetic product after a stereomistake (**8** in both Scheme 5 and Figure 4) is unfavored by 1.7 and 3.2 kcal/mol, respectively, in CH_2Cl_2 and by 1.6 and 2.9 kcal/mol in toluene, with respect to the *S*-metal/*re*-chain product after a correct enantiofacial addition or, equivalently, to the *R*-metal/*si*-chain thermodynamic product (**11** in both Scheme 5 and Figure 4) that can be reached after site epimerization. The energy difference of 3.2 kcal/mol in the presence of the counterion in CH_2Cl_2 substantially replicates the energy difference we calculated in its absence for the (CGC)Ti system (see Figure 2). The assistance of the counterion or a MMA molecule results in a very smooth energy profile for the site epimerization reaction, since the two intermediates without a back-bonded C═O group (**9** and **10** in both Scheme 5 and Figure 4) are remarkably stabilized by a tightly bound counterion or a temporarily coordinated MMA molecule. Further, substitution of the coordinated C═O of the last unit of the chain from the C═O of a MMA molecule results in a rather flat energy profile, whereas displacement by the counterion is less favored, which suggests that the C═O group coordinates better to the metal than the counterion. Further evidence of the preferential coordination of the C═O group to the metal with respect to coordination of the counterion is obtained by a comparison between **8** and **9** in the counterion-assisted site epimerization pathway. Both in toluene and in CH_2Cl_2 the preferred situation is an outer-sphere ion pair with a back-bonding of the last C═O group, structure **8**, rather than an inner-sphere ion pair with no back-bonding from C═O groups of the PMMA chain, structure **9**. This preference is higher in the more polar CH_2Cl_2 solvent, 9.4 in CH_2Cl_2 vs 7.1 kcal/mol in toluene, since the counterion/cation interaction is mainly electrostatic in nature and is thus reduced in more polar solvents.

To investigate in more detail the relative strength of the C═O···Ti and $[MeB(C_6F_5)_3^-]$···Ti interactions as well as their dependence on solvent effects, we calculated the binding energy of a MMA molecule and of the $MeB(C_6F_5)_3^-$ counterion to the (CGC)Ti−OMe^+ system. The presence of a simple methoxy group bonded to the metal avoids any complicacy connected to the removal of a back-bonded C═O and/or to the different steric hindrance of the MMA molecule and of the $MeB(C_6F_5)_3^-$ counterion. Our calculations indicate that in the low polar toluene solvent the $MeB(C_6F_5)_3^-$ counterion is bound to the metal quite more strongly than MMA (45.7 vs 30.1 kcal/mol). Increasing the polarity of the solvent results in a sharp decrease of the binding energy of the $MeB(C_6F_5)_3^-$ counterion (from 45.7 to 23.4 kcal/mol on going from toluene to CH_2Cl_2), which is reasonable considering that the interaction between the counterion and the catalyst, as previously indicated, is mainly electrostatic in nature. The binding energy of the MMA molecule, instead, is substantially independent from the polarity of the medium (from 30.1 to 27.3 kcal/mol on going from toluene to CH_2Cl_2).

Scheme 5

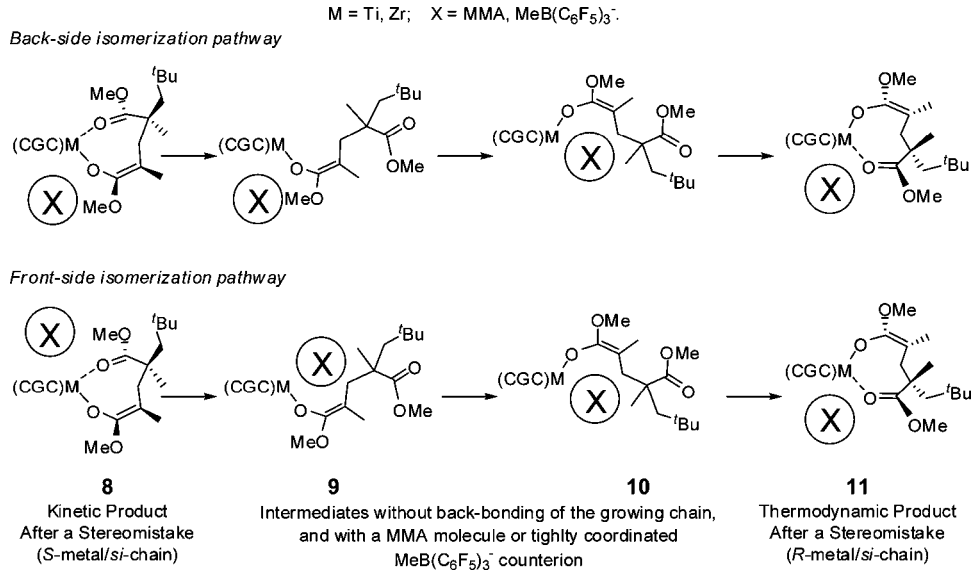

These findings support the main mechanistic scenario which emerged from the experiments. That is, the presence of the isolated *m* stereomistakes can be explained with catalyst site epimerization *after a stereomistake*, which converts a higher energy kinetic product to a thermodynamically more stable resting state. The driving force for the site epimerization reaction originates from steric interaction between the growing chain after a stereomistake and the Cp′ ligand. As an additional remark, we note that higher stability of the eight-membered cycle after correct enantiofacial additions is also a key to rationalize the formation of highly stereoregular syndiotactic PMMA. In fact, there is no tendency for these systems to undergo catalyst site epimerization after correct enantiofacial addition, which would decrease stereoregularity. This observation highlights another remarkable difference between MMA and propene polymerizations using metallocene-based catalysts.

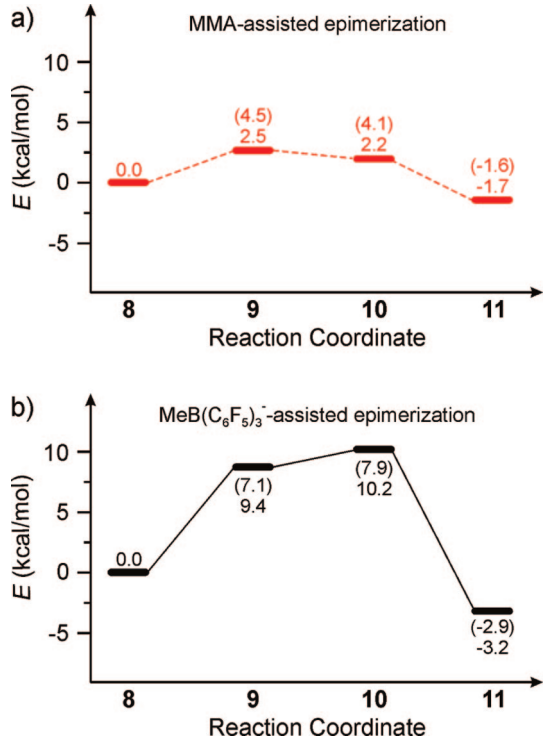

Figure 4. Energy profiles for the site epimerization reaction from the kinetic product after a stereomistake **8** to the thermodynamic resting state **11**. Energies are in kcal/mol, and results are reported for both MMA and counterion-assisted epimerizations in CH_2Cl_2 and toluene.

Conclusions

In summary, the experimental work on the MMA polymerization by the (CGC)M catalysts has revealed additional important features about this polymerization. First, the MMA polymerization by the living/controlled cationic (CGC)Ti alkyl complex **1** follows the zero-order kinetics in MMA concentration; this implies that, in a unimetallic propagation "catalysis" cycle, displacement of the coordinated ester group in the cyclic intermediate by the incoming monomer (ring-opening of the chelate) is fast relative to intramolecular conjugate MMA addition within the catalyst−monomer complex. This observation provides a kinetic basis for pathways leading to catalyst-site epimerization at Ti before MMA additions. Second, there exhibit negligible effects on the syndiotacticity of the polymerization by monomer and catalyst concentrations as well as ion-pairing strength varied with anion structure and solvent polarity. Third, we have synthesized two neutral (CGC)Ti and Zr bis(isopropyl ester enolate) complexes as well as two cationic complexes derived therefrom for the comparative study that required the use of the same bis(ester enolate) complexes. The MMA polymerization results show that both the present (CGC)Ti and Zr ester enolate catalysts are syndioselective at ambient temperature, and the (CGC)Ti system exhibits higher syndioselectivity at this temperature.

On the theoretical side, density functional calculations rationalized the higher syndioselectivity exhibited by the (CGC)Ti catalysts but, more importantly, provided a theoretical support to the catalyst site epimerization mechanism accounting for the formation of the predominately isolated *m* stereoerrors and indicated the driving force for an almost regular site epimerization reaction after a steoreomistake being in the higher energy of the eight-membered cycle formed after a stereomistake. This MMA- or anion-assisted catalyst site epimerization reaction converts the kinetic product after a stereomistake into a thermodynamically more stable resting state.

Acknowledgment. This work was supported by the National Science Foundation (NSF-0718061) for the work carried out at Colorado State University and by Lyondell-Basell Polyolefins and INSTM (Cineca Grant) for the work carried out at the University

of Salerno. We thank Boulder Scientific Co. for the research gifts of $B(C_6F_5)_3$, $[Ph_3C][B(C_6F_5)_4]$, and $[HNMe_2Ph][B(C_6F_5)_4]$.

References and Notes

(1) Selected reviews: (a) Chen, E. Y.-X.; Rodriguez-Delgado, A. In *Comprehensive Organometallic Chemistry III*; Bochmann, M., Vol. Ed.; Mingos, M. P., Crabtree, R. H., Chief Eds.; Elsevier: Oxford, 2007; Vol. *4*, pp 759−1004. (b) Cuenca, T. In *Comprehensive Organometallic Chemistry III*; Bochmann, M., Vol. Ed.; Mingos, M. P., Crabtree, R. H., Chief Eds.; Elsevier: Oxford, 2007; Vol. *4*, pp 323−696. (c) Bochmann, M. *J. Chem. Soc., Dalton Trans.* **1996**, 255–270. (d) Jordan, R. F. *Adv. Organomet. Chem.* **1991**, *32*, 325–387.

(2) Selected books, book chapters, or special journal issues: (a) *Stereoselective Polymerization with Single-Site Catalysts*; Baugh, L. S., Canich, J. A. M., Eds.; CRC Press: Boca Raton, FL, 2008. (b) Resconi, L.; Chadwick, J. C.; Cavallo, L. In *Comprehensive Organometallic Chemistry III*; Bochmann, M., Vol. Ed.; Mingos, M. P., Crabtree, R. H., Chief Eds.; Elsevier: Oxford, 2007; Vol. *4*, pp 1005−1166. (c) Marks, T. J., Ed. *Proc. Natl. Acad. Sci. U.S.A.* **2006**, *103*, 15288−15354, and contributions therein (issue on "Polymerization Special Feature"). (d) Gladysz, J. A., Ed. *Chem. Rev.* **2000**, *100*, 1167−1681, and contributions therein (issue on Frontiers in Metal-Catalyzed Polymerization). (e) Marks, T. J., Stevens, J. C., Eds. *Top. Catal.* **1999**, *7*, 1−208, and contributions therein (issue on Advances in Polymerization Catalysis. Catalysts and Processes). (f) *Metalorganic Catalysts for Synthesis and Polymerization: Recent Results by Ziegler-Natta and Metallocene Investigations*; Kaminsky, W., Ed.; Springer-Verlag: Berlin, 1999. (g) Jordan, R. F., Ed. *J. Mol. Catal. A: Chem.* **1998**, *128*, 1−337, and contributions therein (issue on Metallocene and Single-Site Olefin Catalysts). (h) *Metallocenes: Synthesis−Reactivity−Applications*; Togni A., Halterman, R. L., Eds.; Wiley-VCH: Weinheim, 1998. (i) *Ziegler Catalysts*; Mülhaupt, R., Brintzinger, H.-H., Eds.; Springer-Verlag: Berlin, 1995. (j) Soga, K., Terano, M., Eds. *Stud. Surf. Sci. Catal.* **1994**, *89*, 1−410, and contributions therein (issue on Catalyst Design for Tailor-Made Polyolefins).

(3) Selected reviews: (a) Chen, E. Y.-X. *J. Polym. Sci., Part A: Polym. Chem.* **2004**, *42*, 3395–3403. (b) Boffa, L. S.; Novak, B. M. *Chem. Rev.* **2000**, *100*, 1479–1493.

(4) Ning, Y.; Chen, E. Y.-X. *J. Am. Chem. Soc.* **2008**, *130*, 2463–2465.

(5) Mariott, W. R.; Escudé, N. C.; Chen, E. Y.-X. *J. Polym. Sci., Part A: Polym. Chem.* **2007**, *45*, 2581–2592.

(6) Lian, B.; Thomas, C. M.; Navarro, C.; Carpentier, J.-F. *Organometallics* **2007**, *26*, 187–195.

(7) Ning, Y.; Chen, E. Y.-X. *Macromolecules* **2006**, *39*, 7204–7215.

(8) Rodriguez-Delgado, A.; Mariott, W. R.; Chen, E. Y.-X. *J. Organomet. Chem.* **2006**, *691*, 3490–3497.

(9) Rodriguez-Delgado, A.; Chen, E. Y.-X. *Macromolecules* **2005**, *38*, 2587–2594.

(10) Kostakis, K.; Mourmouris, S.; Kotakis, K.; Nikogeorgos, N.; Pitsikalis, M.; Hadjichristidis, N. *J. Polym. Sci., Part A: Polym. Chem.* **2005**, *43*, 3305–3314.

(11) Ning, Y.; Cooney, M. J.; Chen, E. Y.-X. *J. Organomet. Chem.* **2005**, *690*, 6263–6270.

(12) Lian, B.; Lehmann, C. W.; Navarro, C.; Carpentier, J.-F. *Organometallics* **2005**, *24*, 2466–2472.

(13) Bolig, A. D.; Chen, E. Y.-X. *J. Am. Chem. Soc.* **2004**, *126*, 4897–4906.

(14) Stojcevic, G.; Kim, H.; Taylor, N. J.; Marder, T. B.; Collins, S. *Angew. Chem., Int. Ed.* **2004**, *43*, 5523–5526.

(15) Strauch, J. W.; Fauré, J.-L.; Bredeau, S.; Wang, C.; Kehr, G.; Fröhlich, R.; Luftmann, H.; Erker, G. *J. Am. Chem. Soc.* **2004**, *126*, 2089–2104.

(16) Karanikolopoulos, G.; Batis, C.; Pitsikalis, M.; Hadjichristidis, N. *J. Polym. Sci., Part A: Polym. Chem.* **2004**, *42*, 3761–3774.

(17) Ferenz, M.; Bandermann, F.; Sustmann, R.; Sicking, W. *Macromol. Chem. Phys.* **2004**, *205*, 1196–1205.

(18) Rodriguez-Delgado, A.; Mariott, W. R.; Chen, E. Y.-X. *Macromolecules* **2004**, *37*, 3092–3100.

(19) Lian, B.; Toupet, L.; Carpentier, J.-F. *Chem.−Eur. J.* **2004**, *10*, 4301–4307.

(20) Jensen, T. R.; Yoon, S. C.; Dash, A. K.; Luo, L.; Marks, T. J. *J. Am. Chem. Soc.* **2003**, *125*, 14482–14494.

(21) Chen, E. Y.-X.; Cooney, M. J. *J. Am. Chem. Soc.* **2003**, *125*, 7150–7151.

(22) Mariott, W. R.; Chen, E. Y.-X. *J. Am. Chem. Soc.* **2003**, *125*, 15726–15727.

(23) Jin, J.; Mariott, W. R.; Chen, E. Y.-X. *J. Polym. Sci. , Part A: Polym. Chem.* **2003**, *41*, 3132–3142.

(24) Batis, C.; Karanikolopoulos, G.; Pitsikalis, M.; Hadjichristidis, N. *Macromolecules* **2003**, *36*, 9763–9774.

(25) Karanikolopoulos, G.; Batis, C.; Pitsikalis, M.; Hadjichristidis, N. *Macromol. Chem. Phys.* **2003**, *204*, 831–840.

(26) Bolig, A. D.; Chen, E. Y.-X. *J. Am. Chem. Soc.* **2002**, *124*, 5612–5613.

(27) Jin, J.; Chen, E. Y.-X. *Organometallics* **2002**, *21*, 13–15.

(28) Jin, J.; Wilson, D. R.; Chen, E. Y.-X. *Chem. Commun.* **2002**, *708*, 709.

(29) Jin, J.; Chen, E. Y.-X. *Macromol. Chem. Phys.* **2002**, *203*, 2329–2333.

(30) Bandermann, F.; Ferenz, M.; Sustmann, R.; Sicking, W. *Macromol. Symp.* **2001**, *174*, 247–253.

(31) Karanikolopoulos, G.; Batis, C.; Pitsikalis, M.; Hadjichristidis, N. *Macromolecules* **2001**, *34*, 4697–4705.

(32) Bolig, A. D.; Chen, E. Y.-X. *J. Am. Chem. Soc.* **2001**, *123*, 7943–7944.

(33) Frauenrath, H.; Keul, H.; Höcker, H. *Macromolecules* **2001**, *34*, 14–19.

(34) Nguyen, H.; Jarvis, A. P.; Lesley, M. J. G.; Kelly, W. M.; Reddy, S. S.; Taylor, N. J.; Collins, S. *Macromolecules* **2000**, *33*, 1508–1510.

(35) Bandermann, F.; Ferenz, M.; Sustmann, R.; Sicking, W. *Macromol. Symp.* **2000**, *161*, 127–134.

(36) Cameron, P. A.; Gibson, V.; Graham, A. J. *Macromolecules* **2000**, *33*, 4329–4335.

(37) Stuhldreier, T.; Keul, H.; Höcker, H. *Macromol. Rapid Commun.* **2000**, *21*, 1093–1098.

(38) Chen, E. Y.-X.; Metz, M. V.; Li, L.; Stern, C. L.; Marks, T. J. *J. Am. Chem. Soc.* **1998**, *120*, 6287–6305.

(39) Shiono, T.; Saito, T.; Saegusa, N.; Hagihara, H.; Ikeda, T.; Deng, H.; Soga, K. *Macromol. Chem. Phys.* **1998**, *199*, 1573–1579.

(40) Hong, E.; Kim, Y.; Do, Y. *Organometallics* **1998**, *17*, 2933–2935.

(41) Li, Y.; Ward, D. G.; Reddy, S. S.; Collins, S. *Macromolecules* **1997**, *30*, 1875–1883.

(42) Deng, H.; Shiono, T.; Soga, K. *Macromol. Chem. Phys.* **1995**, *196*, 1971–1980.

(43) Deng, H.; Shiono, T.; Soga, K. *Macromolecules* **1995**, *28*, 3067–3073.

(44) Soga, K.; Deng, H.; Yano, T.; Shiono, T. *Macromolecules* **1994**, *27*, 7938–7940.

(45) Collins, S.; Ward, D. G.; Suddaby, K. H. *Macromolecules* **1994**, *27*, 7222–7224.

(46) Collins, S.; Ward, S. G. *J. Am. Chem. Soc.* **1992**, *114*, 5460–5462.

(47) Lian, B.; Thomas, C. M.; Navarro, C.; Carpentier, J.-F. *Macromolecules* **2007**, *40*, 2293–2294.

(48) Mariott, W. R.; Rodriguez-Delgado, A.; Chen, E. Y.-X. *Macromolecules* **2006**, *39*, 1318–1327.

(49) Kostakis, K.; Mourmouris, S.; Pitsikalis, M.; Hadjichristidis, N. *J. Polym. Sci., Part A: Polym. Chem.* **2005**, *43*, 3337–3348.

(50) Deng, H.; Soga, K. *Macromolecules* **1996**, *29*, 1847–1848.

(51) Miyake, G. M.; Chen, E. Y.-X. *Macromolecules* **2008**, *41*, 3405–3416.

(52) Miyake, G. M.; Mariott, W. R.; Chen, E. Y.-X. *J. Am. Chem. Soc.* **2007**, *129*, 6724–6725.

(53) Mariott, W. R.; Chen, E. Y.-X. *Macromolecules* **2005**, *38*, 6822–6832.

(54) Mariott, W. R.; Chen, E. Y.-X. *Macromolecules* **2004**, *37*, 4741–4743.

(55) Spaether, W.; Klass, K.; Erker, G.; Zippel, F.; Fröhlich, R. *Chem.−Eur. J.* **1998**, *4*, 1411–1417.

(56) Caporaso, L.; Cavallo, L. *Macromolecules* **2008**, *41*, 3439–3445.

(57) Caporaso, L.; Gracia-Budrìa, J.; Cavallo, L. *J. Am. Chem. Soc.* **2006**, *128*, 16649–16654.

(58) Tomasi, S.; Weiss, H.; Ziegler, T. *Organometallics* **2007**, *26*, 2157–2166.

(59) Tomasi, S.; Weiss, H.; Ziegler, T. *Organometallics* **2006**, *25*, 3619–3630.

(60) Hölscher, M.; Keul, H.; Höcker, H. *Macromolecules* **2002**, *35*, 8194–8202.

(61) Hölscher, M.; Keul, H.; Höcker, H. *Chem.−Eur. J.* **2001**, *7*, 5419–5426.

(62) Sustmann, R.; Sicking, W.; Bandermann, F.; Ferenz, M. *Macromolecules* **1999**, *32*, 4204–4213.

(63) (a) Shapiro, P. J.; Cotter, W. D.; Schaefer, W. P.; Labinger, J. A.; Bercaw, J. E. *J. Am. Chem. Soc.* **1994**, *116*, 4623–4640. (b) Okuda, J. *Comments Inorg. Chem.* **1994**, *16*, 185–205. (c) Okuda, J. *Chem. Ber.* **1990**, *123*, 1649–1651. (d) Shapiro, P. J.; Bunel, E.; Schaefer, W. P.; Bercaw, J. E. *Organometallics* **1990**, *9*, 867–869. (e) Piers, W. E.; Shapiro, P. J.; Bunel, E.; Bercaw, J. E. *Synlett* **1990**, *2*, 74–84.

(64) (a) Guo, N.; Stern, C. L.; Marks, T. J. *J. Am. Chem. Soc.* **2008**, *130*, 2246–2261. (b) Motta, A.; Fragalà, I. L.; Marks, T. J. *J. Am. Chem. Soc.* **2007**, *129*, 7327–7338. (c) Gibson, V. C.; Spitzmesser, S. K. *Chem. Rev.* **2003**, *103*, 283–315. (d) Chum, P. S.; Kruper, W. J.; Guest, M. J. *Adv. Mater.* **2000**, *12*, 1759–1767. (e) McKnight, A. L.; Waymouth, R. M. *Chem. Rev.* **1998**, *98*, 2587–2598. (f) Stevens, J. C. *Stud. Surf. Sci. Catal.* **1996**, *101*, 1120; **1994**, *89*, 277−284. (g) Canich, J. A. Eur. Pat. Appl. EP 0420436 A1, **1991**. (h) Stevens, J. C.; Timmers, F. J.; Wilson, D. R.; Schmidt, G. F.; Nickias, P. N.; Rosen, R. K.; Knight, G. W.; Lai, S. Eur. Pat. Appl. EP 0 416815 A2, **1991**.

(65) Allen, R. D.; Long, T. E.; McGrath, J. E. *Polym. Bull.* **1986**, *15*, 127–134.

(66) Feng, S.; Roof, G. R.; Chen, E. Y.-X. *Organometallics* **2002**, *21*, 832–839.
(67) (a) Lee, C. H.; Lee, S. J.; Park, J. W.; Kim, K. H.; Lee, B. Y.; Oh, J. S. *J. Mol. Catal., A: Chem.* **1998**, *132*, 231–239. (b) Biagini, P.; Lugli, G.; Abis, L.; Andreussi, P. U.S. Pat. 5,602269, **1997**.
(68) (a) Resconi, L.; Camurati, I.; Grandini, C.; Rinaldi, M.; Mascellani, N.; Traverso, O. *J. Organomet. Chem.* **2002**, *664*, 5–26. (b) Carpentier, J.-F.; Maryin, V. P.; Luci, J.; Jordan, R. F. *J. Am. Chem. Soc.* **2001**, *123*, 898–909.
(69) Chen, Y.-X.; Marks, T. J. *Organometallics* **1997**, *16*, 3649–3657.
(70) Kim, Y.-J.; Bernstein, M. P.; Galiano Roth, A. S.; Romesberg, F. E.; Williard, P. G.; Fuller, D. J.; Harrison, A. T.; Collum, D. B. *J. Org. Chem.* **1991**, *56*, 4435–4439.
(71) Rodriguez-Delgado, A.; Chen, E. Y.-X. *J. Am. Chem. Soc.* **2005**, *127*, 961–974.
(72) (a) Brar, A. S.; Singh, G.; Shankar, R. *J. Mol. Struct.* **2004**, *703*, 69–81. (b) Bovey, F. A.; Mirau, P. A. *NMR of Polymers*; Academic Press: San Diego, CA, 1996. (c) Kawamura, T.; Toshima, N.; Matsuzaki, K. *Makromol. Chem., Rapid Commun.* **1993**, *14*, 719–724. (d) Chujo, R.; Hatada, K.; Kitamaru, R.; Kitayama, T.; Sato, H.; Tanaka, Y. *Polym. J.* **1987**, *19*, 413–424. (e) Ferguson, R. C.; Ovenall, D. W. *Macromolecules* **1987**, *20*, 1245–1248. (f) Ferguson, R. C.; Ovenall, D. W. *Polym. Prepr.* **1985**, *26*, 182–183. (g) Subramanian, R.; Allen, R. D.; McGrath, J. E.; Ward, T. C. *Polym. Prepr.* **1985**, *26*, 238–240.
(73) (a) ADF2007 *Theoretical Chemistry*, Vrije Universiteit, Amsterdam, **2007**, Users's Manual. (b) Baerends, E. J.; Ellis, D. E.; Ros, P. *Chem. Phys.* **1973**, *2*, 41–51.
(74) Vosko, S. H.; Wilk, L.; Nusair, M. *Can. J. Phys.* **1980**, *58*, 1200–1211.
(75) Becke, A. D. *Phys. Rev. A* **1988**, *38*, 3098–3100.
(76) (a) Perdew, J. P. *Phys. Rev. B* **1986**, *33*, 8822–8824. (b) Perdew, J. P. *Phys. Rev. B* **1986**, *34*, 7406–7406.
(77) (a) Klamt, A.; Schüürmann, G. *J. Chem. Soc., Perkin Trans.* **1993**, 799–805. (b) Pye, C. C.; Ziegler, T. *Theor. Chem. Acc.* **1999**, *101*, 396–408.
(78) Ahlrichs, R.; Bar, M.; Haser, M.; Horn, H.; Kolmel, C. *Chem. Phys. Lett.* **1989**, *162*, 165–169.
(79) Weigend, F.; Ahlrichs, R. *Phys. Chem. Chem. Phys.* **2005**, *7*, 3297–3302.
(80) (a) Haeusermann, U.; Dolg, M.; Stoll, H.; Preuss, H. *Mol. Phys.* **1993**, *78*, 1211–1224. (b) Kuechle, W.; Dolg, M.; Stoll, H.; Preuss, H. *J. Chem. Phys.* **1994**, *100*, 7535–7542. (c) Leininger, T.; Nicklass, A.; Stoll, H.; Dolg, M.; Schwerdtfeger, P. *J. Chem. Phys.* **1996**, *105*, 1052–1059.
(81) Chen, M.-C.; Roberts, J. A. S.; Marks, T. J. *J. Am. Chem. Soc.* **2004**, *126*, 4605–4625.
(82) Ning, Y.; Zhu, H.; Chen, E. Y.-X. *J. Organomet. Chem.* **2007**, *692*, 4535–4544.
(83) Lohrenz, J. C. W.; Woo, T. K.; Ziegler, T. *J. Am. Chem. Soc.* **1995**, *117*, 12793–12800.
(84) Tomasi, S.; Razavi, A.; Ziegler, T. *Organometallics* **2007**, *26*, 2024–2036.

MA801494G